

# Anisotropic finite-size scaling analysis of a three-dimensional driven-diffusive system

Kwan-tai Leung<sup>†</sup> and Jian-Sheng Wang<sup>\*</sup>

<sup>†</sup>*Institute of Physics, Academia Sinica, Nankang, Taipei 11529, Taiwan, Republic of China*

<sup>\*</sup>*Department of Computational Science, National University of Singapore, Singapore 119260, Republic of Singapore*  
(20 May 1998, revised 29 December 1998)

We study the standard three-dimensional driven diffusive system on a simple cubic lattice where particle jumps along a given lattice direction are biased by an infinitely strong field, while those along other directions follow the usual Kawasaki dynamics. Our goal is to determine which of the several existing theories for critical behavior is valid. We analyze finite-size scaling properties using a range of system shapes and sizes far exceeding previous studies. Four different analytic predictions are tested against the numerical data. Binder and Wang's prediction does not fit the data well. Among the two slightly different versions of Leung, the one including the effects of a dangerous irrelevant variable appears to be better. Recently proposed isotropic finite-size scaling is inconsistent with our data from cubic systems, where systematic deviations are found, especially in scaling at the critical temperature.

PACS number(s): 05.50.+q, 64.60.C, 05.70.Jk.

## I. INTRODUCTION

Over the last decade or so, there have been many investigations on nonequilibrium systems. One of the most often studied is the driven diffusive system (DDS) [1] for its simplicity of formulation and richness of novel properties. In particular, it is one of the few simple nonequilibrium systems showing phase transitions similar to that of an equilibrium statistical-mechanical system. The distinction between DDS and an equilibrium system is a subtle one. Although both reach a stationary state of their respective stochastic dynamics in the long time limit, the DDS is generically nonequilibrium, defined only through its dynamics, while an equilibrium system can be alternatively characterized by a Hamiltonian independent of the choice of dynamics. The *standard* DDS model is a lattice gas model governed by Kawasaki dynamics with a driving field. The driving field biases the motion of the particles in one preferred direction, so that under periodic boundary conditions it gives rise to a current along that direction. The existence of a steady current is a manifestation of the nonequilibrium nature of the stationary state. One physical realization of DDS is the superionic conductor. Certain flow properties of binary liquids under gravity, though more complicated due to hydrodynamic modes, are also similar to those of DDS.

In this paper we focus our attention on the critical behavior of the standard DDS. Mean-field theories [2] can give qualitative predictions of the phase transitions. But one of the achievements of the field-theoretic treatment of DDS [3,4] is the exact determination of the set of critical exponents for all dimensions  $d \geq 2$ . After some controversies, the predictions in two dimensions have been confirmed by extensive Monte Carlo simulations [5,6]. The most difficult aspect of such tests is the fact that two length scales are involved—the correlation lengths ( $\xi_{\parallel}$

and  $\xi_{\perp}$ ) diverge differently in direction parallel to the field and in direction perpendicular to the field. Thus, one has to deal with anisotropic finite-size scaling with systems of various geometries.

From a field-theoretic point of view, the  $d = 2$  model is more complicated than in higher dimensions. This is because the usual  $\phi^4$  coupling constant, denoted by  $u$ , is a dangerous irrelevant variable for  $d > 2$ , but it becomes marginal in  $d = 2$ . While scaling arguments can predict the effect of  $u$  on finite-size scaling for  $d > 2$  [5], there is little clue as to the existence and possible form of the associated logarithmic corrections in  $d = 2$ . Perhaps this explains why the agreements between previous tests [5,6] and theory in  $d = 2$  are not impeccable; small deviations from scaling may be due to the presence of small logarithmic corrections. For this reason, a more stringent yet practical test lies in  $d = 3$ .

Recently, not only the confirmations in  $d = 2$  [5,6] but also the validity of the field-theoretic approach itself have been questioned by Marro et al [7]. Isotropic finite-size scaling involving one scaling length was advocated. It is therefore our aim here to try to answer those questions by conducting a comprehensive test of the field-theoretic predictions in  $d = 3$ . Being free from the doubt of possible logarithmic correction, consistencies between simulations and field theory would lend strong support to the latter.

There are very old Monte Carlo simulation results [8,9] of the three-dimensional DDS. One of the discoveries by Monte Carlo as well as by analytic works is the power-law long-range correlation of the particle density even in the high-temperature disordered phase [1,9,10]. This is shown as the manifestation of the violation of the fluctuation-dissipation theorem in DDS. But the question of the validity of the field-theoretic results is far from answered. Monte Carlo simulation of the DDS model

is difficult for its long relaxation times and anisotropic correlations, due to local conservation and the external drive, respectively. In this article, we report a fairly extensive Monte Carlo study using anisotropic finite-size scaling analysis similar to that in the two-dimensional case. A dominant feature of the anisotropies is the appearance of an extra scaling variable, the “aspect ratio”  $S = L_{\parallel}^{1/\lambda}/L_{\perp}$ , with  $\lambda = \nu_{\parallel}/\nu_{\perp}$ . The exponents  $\nu_{\perp}$  and  $\nu_{\parallel}$  are associated with the correlation lengths  $\xi_{\perp}$  and  $\xi_{\parallel}$ . Simple data collapse among different samples is possible only when they have the same value of  $S$ , then the ordinary finite-size scaling forms are valid. There have been different predictions for the value of  $\lambda$ : In  $d = 3$ , field theory predicts that  $\lambda = 8/3$ , whereas Binder and Wang [11] obtained  $\lambda = 4$ . In this work, we mainly concentrate on samples with one fixed  $S$ , using the value  $8/3$  for  $\lambda$ . The results support the field-theoretic predictions. Due to the huge demand on computer power, we could not study extensively the dependence on  $S$ , and the scaling at  $T_c$ , but only have some limited checks. We also test the assumption of isotropic scaling which corresponds to  $\lambda = 1$ . Inconsistencies are found.

## II. THE DDS MODEL AND SIMULATION TECHNIQUE

The model is defined on a simple cubic, fully periodic lattice of size  $L_{\parallel} \times L_{\perp}^2$ . Each site on the lattice has a spin  $\sigma_i = \pm 1$ . Equivalently, we can also consider the system as a lattice gas with local occupation variables. The total magnetization is set exactly at zero, and we assume ferromagnetic interaction among nearest neighbors only, with a coupling constant  $J > 0$ . Equivalently, the particle occupation is half filled and they attract each others. The system evolves according to the standard Kawasaki dynamics of spin exchanges except with an extra ingredient due to an external “electric” field. We associate a positively charged particle with an up spin and a hole with a down spin. Particle hoppings along the electric field are favored. Hereafter we will use the spin language. In simulation, we consider only the extreme case of infinitely strong field, chosen to be in the  $+x$  direction. Thus, exchange is always performed if we have a  $(+, -)$  pair along the  $+x$  direction and the exchange for  $(-, +)$  is forbidden. When the exchanges are perpendicular to the field (which happens 2/3 of the time), the field does not play any role. In that case, we compute the change in energy  $\Delta E$  due to the exchange, accepting it with the Metropolis rate  $\min(1, \exp(-\Delta E/kT))$ . From now on, we will set  $J/k$  to one.

Since the model evolves very slowly via a conservative dynamics, a fast algorithm is of the utmost importance for the present undertaking. We used a multi-spin coded program to simulate 8 or 16 systems simultaneously, depending on the word length of the given machine. The method is similar to that of Kawashima et al [12], capa-

ble of achieving a speed of about  $0.1 \mu\text{sec}/(\text{spin flip})$  with a typical workstation.

We define the order parameter as

$$\phi = \frac{1}{2L_{\parallel}L_{\perp}} \sin\left(\frac{\pi}{L_{\perp}}\right) \sqrt{|\tilde{\sigma}(0, 1, 0)|^2 + |\tilde{\sigma}(0, 0, 1)|^2}, \quad (1)$$

where

$$\tilde{\sigma}(l, m, n) = \sum_{x=0}^{L_{\parallel}-1} \sum_{y=0}^{L_{\perp}-1} \sum_{z=0}^{L_{\perp}-1} \sigma_{x,y,z} e^{\frac{2\pi i l x}{L_{\parallel}}} e^{\frac{2\pi i (m y + n z)}{L_{\perp}}}. \quad (2)$$

The normalization is chosen such that  $\phi = 1$  for a slab geometry (the completely phase-separated configuration in the limit  $T \rightarrow 0$ ). The following quantities are calculated: (i) the averaged order parameter  $m = \langle \phi \rangle$ , (ii) the “susceptibility” proportional to the fluctuation of the order parameter,

$$\chi = \frac{L_{\parallel}L_{\perp}}{T \sin(\pi/L_{\perp})} \left[ \langle \phi^2 \rangle - \langle \phi \rangle^2 \right], \quad (3)$$

the susceptibility above the critical temperature,

$$\chi' = \frac{L_{\parallel}L_{\perp}}{T \sin(\pi/L_{\perp})} \langle \phi^2 \rangle, \quad (4)$$

and (iii) the fourth-order cumulant,

$$g = 2 - \frac{\langle \phi^4 \rangle}{\langle \phi^2 \rangle^2}. \quad (5)$$

Note that  $g$  goes from 0.5 to 1 as temperature  $T$  goes from  $\infty$  to 0. We will not report the results on  $\chi'$ ; it yields no additional information as  $\langle \phi^2 \rangle$  appears to scale like  $\langle \phi \rangle^2$ .

The computations are performed on a variety of workstations, such as Alpha-stations, Pentium clusters, IBM SP2, etc. Our main results are obtained from a set of system sizes  $(L_{\parallel}, L_{\perp})$  with (113, 18), (193, 22), (367, 28), and (524, 32), chosen such that  $S = L_{\parallel}^{3/8}/L_{\perp}$  is very close to a constant, ranging between 0.32703 to 0.32709. A second set with (59, 35), (102, 43), (122, 46), (161, 51), and (248, 60) are used mainly to confirm the result for  $T_c$ . The value of  $S$  for this set varies from 0.13171 to 0.13182. Much more elongated geometries are also used to investigate the  $L_{\parallel} \rightarrow \infty$  behavior. A third set with cubic geometry,  $L = L_{\perp} = L_{\parallel} = 20, 30, 40, 50, 60$ , is used to test isotropic scaling. The lengths of runs are  $10^6$  to  $10^8$  Monte Carlo steps per temperature, the longer for  $T$  closer to  $T_c$ . We monitor the results until the system is well equilibrated before actually taking data. The total amount of CPU time spent is of the order of seven years on one IBM SP2 node. This gives an idea of the computational demand in achieving good statistics for this model.

### III. ANISOTROPIC FINITE-SIZE SCALING

There have been two competing theories on the anisotropic finite-size scaling of the DDS. The first is that of Binder and Wang [11]. Their results are based on a generalization of the one-dimensional Ginzburg-Landau type effective Hamiltonian for the very elongated geometry. The second is due to Leung based on the field-theoretic formulation [5].

Encouraged by the finite-size scaling of the standard Ising model above its upper critical dimension and the finite-size scaling at a Lifshitz point, Binder and Wang [11] speculated on a scaling form for the driven diffusive model. The starting point is the assumption of an effective functional for the local order parameter  $\Psi$  in a quasi-one-dimensional geometry ( $L_\perp \ll L_\parallel$ ),

$$H_{eff}(\Psi) = L_\perp^{d-1} \int_0^{L_\parallel} dz \left[ \frac{1}{2} \left( \frac{d^\kappa \Psi}{dz^\kappa} \right)^2 + \frac{1}{2} t \Psi^2 + \frac{u_0}{4!} \Psi^4 \right], \quad (6)$$

where the exponent  $\kappa^{-1} = 2 + (5-d)/3$  which characterizes the singular term is introduced in such a way that the correlation-length exponent  $\nu_\parallel$  as obtained by field theory is reproduced at the Gaussian level. This leads to the scaling forms for the susceptibility and magnetization in three dimensions [11] at  $T = T_c$

$$\chi(T_c) = L_\parallel^{3/4} \tilde{\chi}(L_\parallel^{1/4}/L_\perp), \quad (7)$$

$$m(T_c) = L_\parallel^{-3/8} \tilde{m}(L_\parallel^{1/4}/L_\perp). \quad (8)$$

On the other hand, Leung deduced the off- $T_c$  finite-size scaling forms by generalizing the exact field-theoretic results for infinite system sizes to finite sizes [5]. The derivation was based on a combination of the renormalization group argument which treats  $1/L_\perp$  and  $1/L_\parallel$  as two independent relevant variables, and scaling arguments which assume multiplicative singularities in the limit  $u L_\parallel^{-2\theta/\lambda} \rightarrow 0$ . Here  $\theta$  is proportional to the anomalous dimension of  $u$ . The fact that  $\theta = 1 - (5-d)/3 \geq 0$  for  $d \geq 2$  prescribes the dangerous nature of  $u$  above two dimensions. The main results read [5]

$$\chi(T) = L_\parallel^{7/8} \tilde{\chi}(L_\parallel^{3/8}/L_\perp, t L_\parallel^{7/8}), \quad (9)$$

$$m(T) = L_\parallel^{-7/16} \tilde{m}(L_\parallel^{3/8}/L_\perp, t L_\parallel^{7/8}), \quad (10)$$

$$g(T) = \tilde{g}(L_\parallel^{3/8}/L_\perp, t L_\parallel^{7/8}), \quad (11)$$

where  $t = (T - T_c)/T_c$ . If the contribution from the dangerous irrelevant variable  $u$  was ignored, we would have instead

$$\chi(T) = L_\parallel^{3/4} \tilde{\chi}(L_\parallel^{3/8}/L_\perp, t L_\parallel^{3/4}), \quad (12)$$

$$m(T) = L_\parallel^{-1/2} \tilde{m}(L_\parallel^{3/8}/L_\perp, t L_\parallel^{3/4}), \quad (13)$$

$$g(T) = \tilde{g}(L_\parallel^{3/8}/L_\perp, t L_\parallel^{3/4}). \quad (14)$$

The above results imply that the thermodynamic limit has to be taken carefully. The field-theoretic results are understood to correspond to the case where  $L_\parallel \propto L_\perp^\lambda \rightarrow \infty$ . Besides this limit, the quasi-one-dimensional limit  $L_\parallel \rightarrow \infty$  with  $L_\perp$  held finite is also of interest (we assume that there exists a unique value of  $T_c$  for these different ways of taking the thermodynamic limit.) Since  $\chi$  does not depend on  $L_\parallel$  in this case, from Eqs. (7), (9) and (12), we have three different predictions for the susceptibility at  $T_c$

$$\text{Binder \& Wang} \quad \chi \sim L_\perp^3, \quad (15)$$

$$\text{Leung (with } u) \quad \chi \sim L_\perp^{7/3}, \quad (16)$$

$$\text{Leung (without } u) \quad \chi \sim L_\perp^2. \quad (17)$$

We will use Eqs. (7)-(17) to check which version of the predictions for scaling describes the data of computer simulation better.

### IV. ANISOTROPIC SCALING RESULTS

An accurate determination of the critical temperature  $T_c$  is important for a quantitative analysis of the critical behavior. We determine  $T_c$  by the finite-size effect of the location  $T_{\text{peak}}$  of the susceptibility peak in  $\chi$ . The data near peaks are fitted with a parabola to derive their heights and locations. First we consider the predictions in Eqs. (9) and (12). Following well-known argument, the shift of  $T_c$  due to finite sizes is

$$T_{\text{peak}}(L_\parallel, S) = T_c + a(S) L_\parallel^{-b}, \quad (18)$$

where  $a(S)$  is a scaling function,  $b = 7/8$  or  $3/4$ . When  $S = L_\parallel^{3/8}/L_\perp$  is fixed, we have the usual shift of the peak locations. Fig. 1(a) shows  $T_{\text{peak}}$  against  $L_\parallel^{-7/8}$ , for two sets of data with  $S = 0.327$  (first set, lower part) and  $S = 0.1317$  (second set, upper part), respectively. Least-square fit extrapolates to critical temperatures  $4.859 \pm 0.005$  (first set) and  $4.869 \pm 0.005$  (second set). If the exponent  $3/4$  is used in Eq. (18), according to Eq. (12), the estimate shifts to higher values of  $4.870 \pm 0.005$  (first set)  $4.873 \pm 0.005$  (second set). Thus, while the extrapolated  $T_c$  from the two sets of data agree within errors for both versions, the one with the exponent  $3/4$  without the dangerous irrelevant variable correction appears to be marginally more consistent. The consistency in  $T_c$  for two different sets of data with fixed  $S$

is a significant confirmation that  $\lambda = 8/3$  is the correct anisotropic scaling exponent.

The peak heights are additional information which we can use. According to Eq. (9) and (12), the peak height scales with system size as  $\chi_{\max} \sim L_{\parallel}^{7/8}$  or  $\chi_{\max} \sim L_{\parallel}^{3/4}$  if the variable  $u$  is or is not taken into account. The nice feature of the susceptibility maximum scaling is that it does not depend on the choice of the second scaling variable  $tL_{\parallel}^c$  in the scaling functions. In Fig. 2, we plot the height vs.  $L_{\parallel}$  in logarithmic scale. The insert shows shift of the susceptibility peaks. Very nice linear behavior with a slope of  $0.86 \pm 0.02$  is obtained. This is a solid confirmation of Eq. (9).

For fixed  $S$ , the anisotropic finite-size scaling has the same form as the isotropic scaling, involving a prefactor in  $L$  and just one scaling variable of the form  $tL^c$ . We first look at the scaling of the fourth order cumulant. This quantity has a simple scaling since there is no prefactor. Fig. 3(a) is the cumulant  $g$  plotted against scaling variable  $tL_{\parallel}^{7/8}$ . If the dangerous irrelevant variable  $u$  was ignored, the exponent  $c$  would be  $3/4$ . The corresponding scaling plot is Fig. 3(b). Both of them yield equally well data collapsing if different  $T_c$  are used.

The finite-size scaling of the order parameter is presented in Fig. 4. Excellent scaling is found there when  $u$  is taken into account, using Eq. (10). The upper branch is for  $t < 0$  and the lower branch is for  $t > 0$ . Fig. 3(a) shows that the upper branch has a slope of about 0.5 for large value of  $tL_{\parallel}^{7/8}$ , which is consistent with the exponent  $\beta = 1/2$ . If  $u$  is ignored, using Eq. (13) instead, Fig. 3(b) shows that the data collapse is not as good below  $T_c$ .

The susceptibility data are shown in Fig. 5 in scaling form. The upper curve with a peak is for  $t < 0$  and the lower curve is for  $t > 0$ . The scaling is not as good as that for the order parameter at low temperatures. A plausible explanation for such deviations from scaling is that the low- $T$  data may fall outside the critical region. If this is the case, the size of the critical region could then be estimated to be about 10% of  $T_c$ . This interpretation is supported by the same kind of deviation in the low- $T$  tails in  $\chi$  and  $m$  in equilibrium Ising model [13], where the exponents are known exactly and thus cannot be the source of deviations. Similar behavior is also found in two-dimensional DDS [6].

We now turn our attention to finite-size scaling at  $T_c$ , where only one scaling variable of the form  $L_{\parallel}^{1/\lambda}/L_{\perp}$  is left. We simulate a wide range of system sizes and shapes, no longer restricting to ones with fixed  $L_{\parallel}^{3/8}/L_{\perp}$ . The exponent  $\lambda$  can be determined when ensemble averages for different  $(L_{\parallel}, L_{\perp})$  fall on one curve when plotted against  $L_{\parallel}^{1/\lambda}/L_{\perp}$ . Since large systems take very long time to equilibrate at  $T_c$ , we do not have very precise data. Nevertheless, it is sufficient to distinguish among alternative predicted scaling forms. First, the fourth-order cumulant

at  $T_c = 4.860$  is presented in Fig. 6. The prediction of Leung with or without  $u$  term has the same scaling variable  $L_{\parallel}^{3/8}/L_{\perp}$ , while that of Binder and Wang is  $L_{\parallel}^{1/4}/L_{\perp}$ . Isotropic scaling variable is  $L_{\parallel}/L_{\perp}$ . The three sets of curves correspond to these three cases. Leung's scaling appears better. This plot also shows that for  $S \approx 0.14$  we get a maximum value in  $g$ . This value corresponds to geometries where two correlation lengths have the same ratio to the respective linear dimensions. For the assumption of  $L_{\parallel}/L_{\perp}$  as scaling variable, the data clearly do not scale well. This appears to be a strong evidence in favor of anisotropic scaling. The same type of plots assuming  $T_c = 4.872$  does not give good scaling for all the choices of the scaling variables. This seems to imply that  $T_c = 4.860$  is a better estimate for the critical temperature.

In Fig. 7 we show the scaling of magnetization at  $T_c = 4.860$ . Fig. 7(a) uses Binder and Wang scaling, (b) Leung's scaling with  $u$  correction, and (c) without  $u$  correction. Case (a) has large deviations; case (b) generally scales better except at large  $L_{\parallel}^{3/8}/L_{\perp}$ . The scaling assuming  $T_c = 4.872$  (not shown) looks worse for case (a), and better for (c) at large scaling variable. Case (b) scales the best in both temperatures. This shows that the relative quality of scaling is not sensitive to the choice of  $T_c$  within its extrapolated range. The scaling function  $\tilde{m}(x)$  has the following asymptotic behaviors at large  $L_{\parallel}$  or  $L_{\perp}$  limit due to the sum of magnetization of totally independent regions. For small  $x$ ,  $m \propto 1/L_{\perp}$ , this implies  $\tilde{m}(x) \sim x$  for all three cases. for large  $x$ , we have  $m \propto 1/L_{\parallel}^{1/2}$ , thus  $m(x) \sim x^y$ ,  $y = -1/2, -1/6, 0$ , respectively for case (a), (b), and (c). Unfortunately, all three plots are more or less consistent with this asymptotic slopes and thus alone it cannot give a sensitive test.

Fig. 8 show the corresponding scaling plots for the susceptibility at the same choice of  $T_c$ . The trend is the same as in  $m$ . Although all three cases satisfy Eqs. (15)–(17) for large  $L_{\parallel}^{1/\lambda}/L_{\perp}$ , case (b) is most consistent with the notion of a scaling function  $\tilde{\chi}(x)$ .

Finally, in Fig. 9, we do a separate test of the predictions of Eqs. (15)–(17) for the very long geometry ( $L_{\parallel} \rightarrow \infty$ ,  $L_{\perp}$  finite). The critical temperature is taken to be  $T_c \approx 4.860$ . The  $L_{\parallel} \rightarrow \infty$  limit is obtained by systems (1280,20), (960,30), (320,40) together with smaller systems and extrapolated to large  $L_{\parallel}$ , assuming a  $1/L_{\parallel}$  convergence or similar power. The least-square fit to the data in Fig. 9 gives exponent  $2.27 \pm 0.07$ , in good agreement with Leung's scaling with  $u$  taken into account. However, if  $T_c = 4.872$  is used, the exponent reduces to  $2.04 \pm 0.09$ . Thus the distinction with or without  $u$ -correction is not clear cut. On the other hand, Binder and Wang's scaling requires the exponent to be 3. This seems unlikely to be satisfied, due to the lack of data collapse in Fig. 8(a). This demonstrates that to pass a consistency check at  $T_c$  requires both a good data collapse and the correct asymptotic behaviors.

## V. ISOTROPIC SCALING

There have been arguments [14] that DDS under infinitely large driving field could follow the normal isotropic finite-size scaling with one single correlation length exponent, although no specific prediction of scaling exponents are given. For completeness, we test it by analyzing cubic systems with  $L = 20, 30, 40, 50$ , and  $60$ , assuming the usual finite-size scaling:

$$\chi(T) = L^{\gamma/\nu} \tilde{\chi}(tL^{1/\nu}), \quad (19)$$

$$m(T) = L^{-\beta/\nu} \tilde{m}(tL^{1/\nu}), \quad (20)$$

$$g(T) = \tilde{g}(tL^{1/\nu}). \quad (21)$$

A second scaling variable  $L_{\parallel}/L_{\perp}$ , equal to one in our data, is not explicitly written. In Fig. 10, we plot the location  $T_{\text{peak}}$  of the susceptibility peak versus  $L^{-1/\nu}$  with two choices of  $\nu$ . Values of  $\nu$  outside this range result in unacceptable, nonlinear behavior. This plot therefore gives us an idea of the bounds of  $T_c$ . Peak extrapolation depends on the assumption on  $\nu$ , varying from 4.86 to 4.90 for  $\nu = 0.67$  to  $1$ . The curve is not quite linear for any choice of  $\nu$ ; this is expected if the true behavior is given by Eq. (18). The insert shows the intersections of the fourth-order cumulant. The intersections shift towards higher values from 4.83 to 4.86 as  $L$  increases. If we trust the larger system sizes, the estimate of  $T_c$  would be 4.86. This is the value barely in agreement with the extrapolation.

Having determined  $T_c$ , the best off- $T_c$  scaling is seen in  $m$ , achieved by choosing  $T_c = 4.863$ ,  $1/\nu = 1.53$ , and  $\beta/\nu = 0.638$  (see Fig. 11). However, this set of parameters is not the best choice for  $g$ . Figure 12 shows that with the same  $T_c$  and  $\nu$  as for  $m$ . Due to the fact that  $g$  curves are not intersecting at a unique  $T$ , systematic deviations are observed no matter what values of  $T_c$  and  $\nu$  are used. Next, we determine  $\gamma/\nu = 1.81$  from the susceptibility peak height vs. system size. Relatively large deviation also occurs for the off- $T_c$  susceptibility data (Fig. 13).

Even though the data more or less scale in  $tL^{1/\nu}$  with a suitable set of exponents, we see systematic deviations and slight inconsistency among different quantities. The quality of data collapsing is inferior to that of the anisotropic scaling except perhaps for  $m$ . Since the critical temperature estimated from isotropic scaling agrees with that of anisotropic scaling, the same data obtained for the purpose of testing anisotropic scaling at  $T_c$  can also be used to test isotropic scaling. The results do not support the latter. We have already seen that the fourth order cumulant  $g$  does not scale (Fig. 6,  $a = 1$ ). In Fig. 14 we show  $mL_{\perp}^{\beta/\nu}$  vs.  $L_{\parallel}/L_{\perp}$  at  $T_c$ . If the system is isotropic, it should scale. But clearly, we see large systematic deviations. Finally, in the quasi-one-dimensional limit, the equation analogous to Eqs. (15)–(17) is  $\chi \propto L_{\perp}^{\gamma/\nu} = L_{\perp}^{1.8}$ , but the actual exponent from the data is much larger (Fig. 9).

The reason for the above good fits off  $T_c$  and the poor fits at  $T_c$  is a consequence of our fitting the former first. This warrants the crossing at  $L_{\parallel}/L_{\perp} = 1$  in Fig. 14. The fact that there is no collapse elsewhere along the  $L_{\parallel}/L_{\perp}$  axis is a clear indication of the failure of the assumption of isotropic scaling. Thus, the moral of this exercise is that an apparently good fit from a partial test may be dangerously misleading in the case of scaling with two variables.

## VI. CONCLUSION

We have performed a large-scale simulation for the standard driven diffusive model. We test the theoretical predictions of finite-size scaling against numerical data, as carefully, critically and completely as we can. The task is to decide which of the various competing theories is the most consistent with the data. There have been four theoretical proposals, characterized by different sets of finite-size scaling exponents. Two kinds of scaling tests are performed: at and off the critical temperature. Both are necessary because there are two scaling variables involved. The two versions due to Leung, with and without the dangerous irrelevant variable correction, fit the off- $T_c$  data almost equally well if  $T_c$  is adjusted accordingly. As to the data taken at  $T_c$ , while they do not have enough quality for us to perform a stringent test, the scaling behavior and susceptibility peak heights clearly favor the one including the dangerous irrelevant variable. Such tests also indicate that Binder and Wang scaling may not be valid. Regarding the recent proposal based on isotropic scaling, we find that the data can be cast in scaling forms with some effective exponents, but its theoretical basis is more conjectural, and the quality of scaling is poorer especially at  $T_c$ . Thus, taking into account all aspects of scaling, we conclude that the field-theoretic prediction based on spatial anisotropies with dangerous irrelevant variable corrections is the most satisfactory.

## ACKNOWLEDGMENT

The work of JSW was supported in part by an Academic Research Grant No. RP950601. KtL acknowledges supports by the National Science Council of ROC through grants NSC87-2112-M-001-006 and NSC88-2112-M-001-013, and a Main-theme grant from the Academia Sinica.

- 
- [1] B. Schmittmann, *Int. J. Mod. Phys. B* **4**, 2269 (1990); B. Schmittmann and R. K. P. Zia, in *Phase Transitions*

- and *Critical Phenomena*, Vol 17, edited by C. Domb and J. L. Lebowitz (Academic Press, New York, 1995).
- [2] R. Dickman, *Phys. Rev. B*, **38**, 2588 (1988); N. C. Peshcheva, Y. Shnidman, and R. K. P. Zia, *J. Stat. Phys.* **70**, 737 (1993).
  - [3] H. K. Janssen and B. Schmittmann, *Z. Phys. B* **64**, 503 (1986).
  - [4] K.-t. Leung and J. Cardy, *J. Stat. Phys.* **44**, 567 (1986) and **45**, 1087 (1986).
  - [5] K.-t. Leung, *Phys. Rev. Lett.* **66**, 453 (1991); K.-t. Leung, *Int. J. Mod. Phys. C* **3**, 367 (1992).
  - [6] J.-S. Wang, *J. Stat. Phys.* **82**, 1409 (1996).
  - [7] J. Marro, A. Achahbar, P.L. Garrido and J.J. Alonso, *Phys. Rev. E* **53**, 6038 (1996); and *J. Stat. Phys.* **78**, 1493 (1995).
  - [8] J. Marro, J. L. Vallés, and J. M. Gonzalez-Miranda, *Phys. Rev. B* **35**, 3372 (1987).
  - [9] M. Q. Zhang, J.-S. Wang, J. L. Lebowitz, and J. L. Vallés, *J. Stat. Phys.* **52**, 1461 (1988).
  - [10] P. L. Garrido, J. L. Lebowitz, C. Maes, and H. Spohn *Phys. Rev. A* **42**, 1954 (1990).
  - [11] K. Binder and J.-S. Wang, *J. Stat. Phys.* **55**, 87 (1989).
  - [12] N. Kawashima, N. Ito, and Y. Kanada *Int. J. Mod. Phys. C* **4**, 525 (1993).
  - [13] K.-t. Leung and R.K.P. Zia, *J. Stat. Phys.* **83**, 1219 (1996).
  - [14] F. de los Santos and P. L. Garrido, cond-mat/9805211 (preprint, 1998).

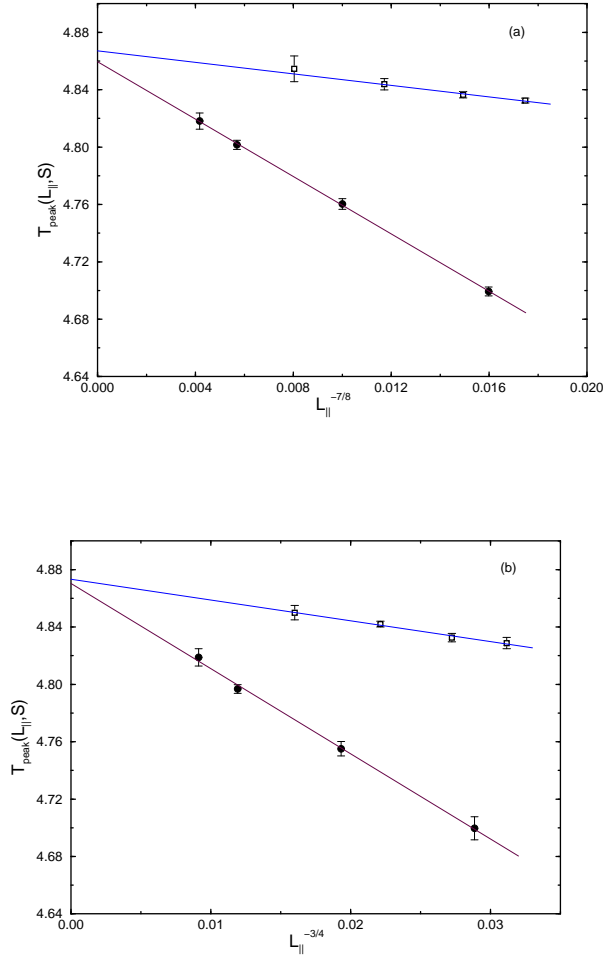


FIG. 1. The susceptibility peak location  $T_{\text{peak}}(L_{\parallel}, S)$  as a function of  $L_{\parallel}^{-b}$ ; (a)  $b = 7/8$ , (b)  $b = 3/4$ . The system sizes  $(L_{\parallel}, L_{\perp})$  are (113,18), (193,22), (367,28), (524,32) [solid circle]; and (102,43), (122,46), (161,51), (248,60) [open square]. The limiting value  $T_{\text{peak}}(L_{\parallel} \rightarrow \infty, S)$  is an estimate of  $T_c$ .

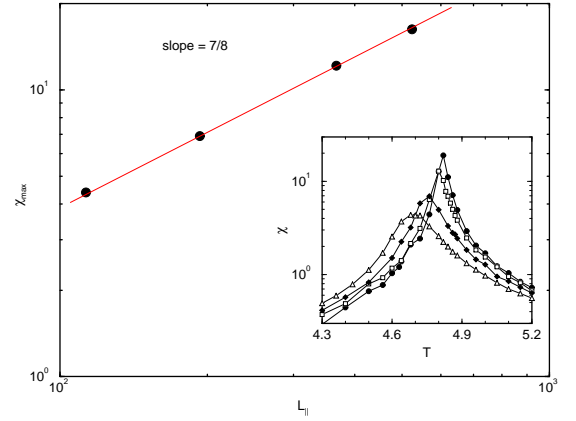


FIG. 2. Scaling of the susceptibility maxima. The slope is as predicted in Eq. (9), within error from the best fit 0.86. The insert shows the shift of the susceptibility peaks for  $(L_{\parallel}, L_{\perp})$  being (113,18), (193,22), (367,28), and (524,32) from left to right.

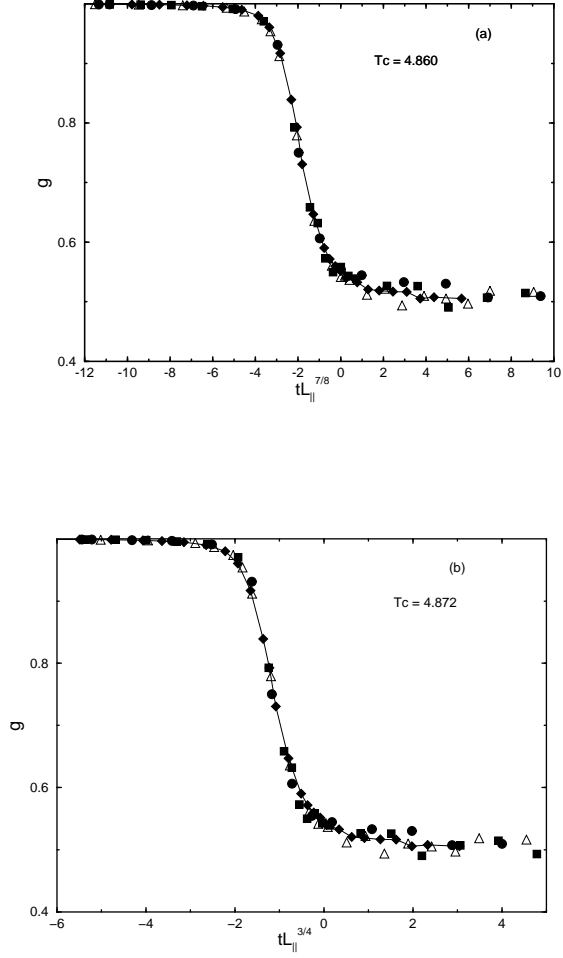


FIG. 3. The finite-size scaling of the fourth order cumulant  $g$  with the scaling variable (a)  $tL_{\parallel}^{7/8}$  and  $T_c = 4.860$ ; and (b)  $tL_{\parallel}^{3/4}$  and  $T_c = 4.872$ . The system sizes  $(L_{\parallel}, L_{\perp})$  are (113,18) [diamond], (193,22) [triangle], (367,28) [square], (524,32) [circle].

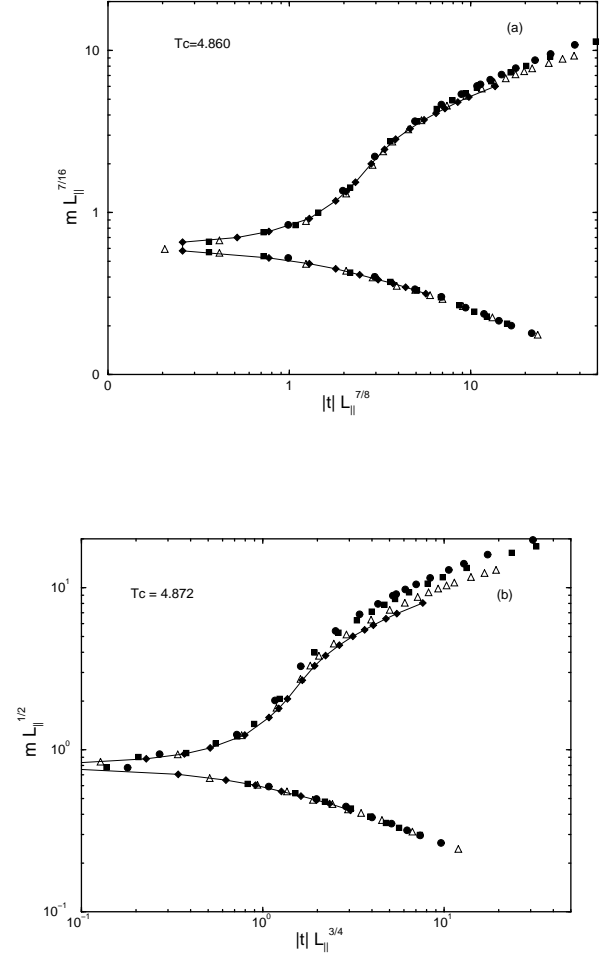


FIG. 4. The finite-size scaling of the order parameter  $m$  with the scaling variable (a)  $tL_{\parallel}^{7/8}$  and  $T_c = 4.860$ ; and (b)  $tL_{\parallel}^{3/4}$  and  $T_c = 4.872$ . The system sizes are the same as in the previous figure.



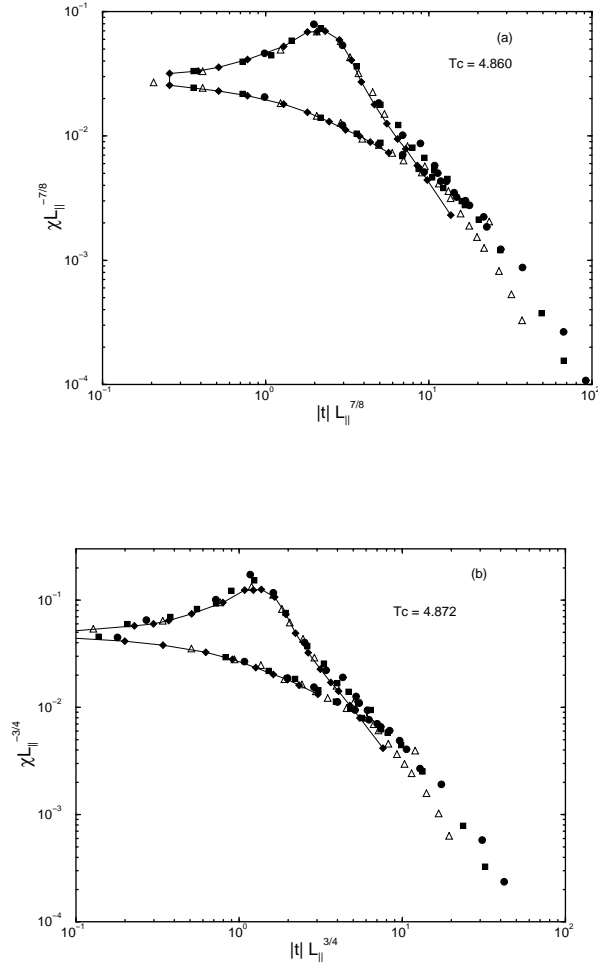


FIG. 5. The finite-size scaling of the susceptibility  $\chi$  with the scaling variable (a)  $tL_{\parallel}^{7/8}$  and  $T_c = 4.860$ ; and (b)  $tL_{\parallel}^{3/4}$  and  $T_c = 4.872$ . The system sizes are the same as in the previous figure.

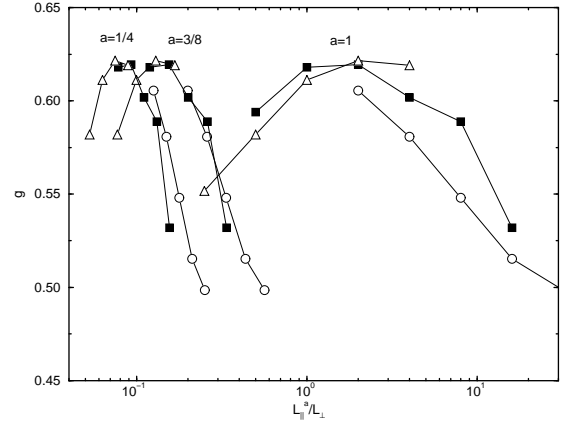


FIG. 6. The scaling of the fourth-order cumulant at  $T_c = 4.860$ . The left set of curves with  $a = 1/4$  refers to the prediction of Binder and Wang; the middle set with  $a = 3/8$  is that of Leung; the right set assumes isotropic scaling  $a = 1$ . Same symbol means the same transverse system size  $L_{\perp} = 40, 30$  and  $20$ , from left to right.

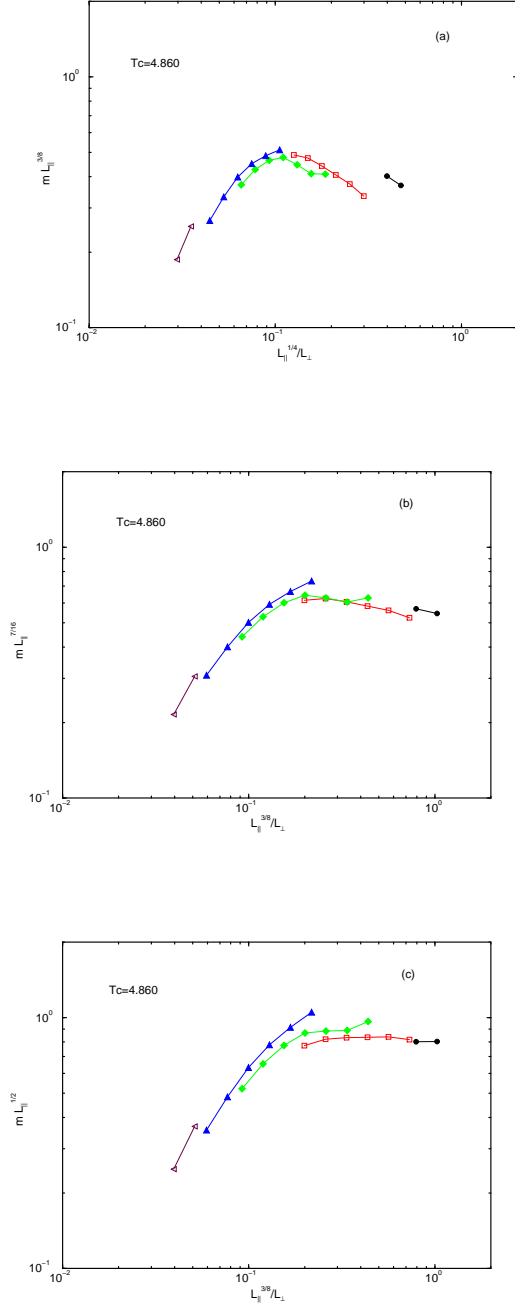


FIG. 7. The finite-size scaling of magnetization at  $T_c = 4.86$  for (a) Binder and Wang scaling; (b) Leung scaling with  $u$ ; (c) Leung scaling without  $u$ . Same symbol means the same transverse system size  $L_\perp = 60, 40, 30, 20$  and  $10$ , from left to right.

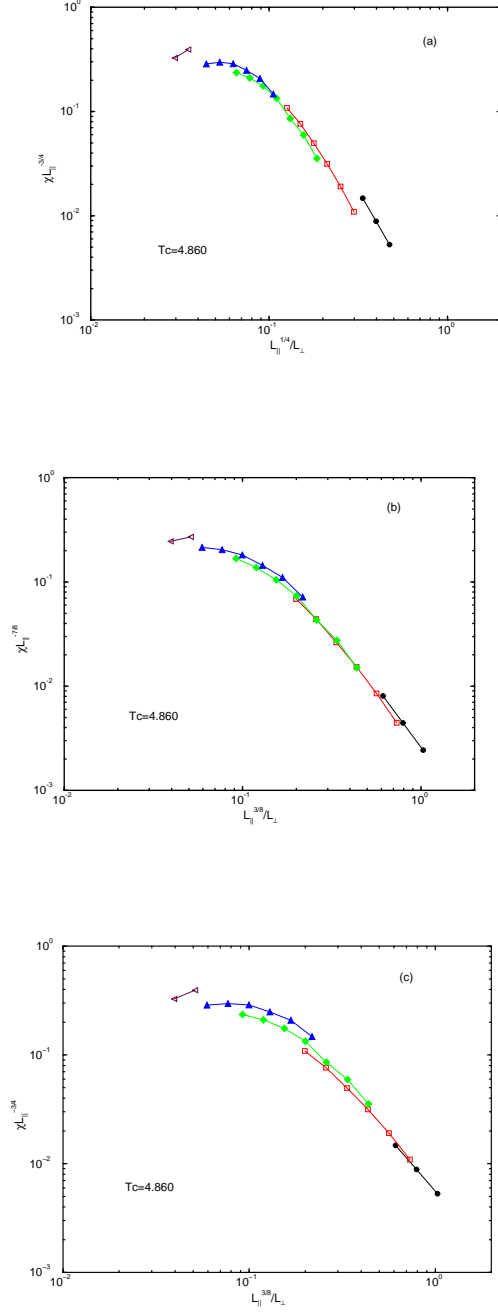


FIG. 8. The finite-size scaling of susceptibility at  $T_c = 4.86$  for (a) Binder and Wang scaling; (b) Leung scaling with  $u$ ; (c) Leung scaling without  $u$ . Same symbol means the same transverse system size  $L_\perp = 60, 40, 30, 20$  and  $10$ , from left to right.

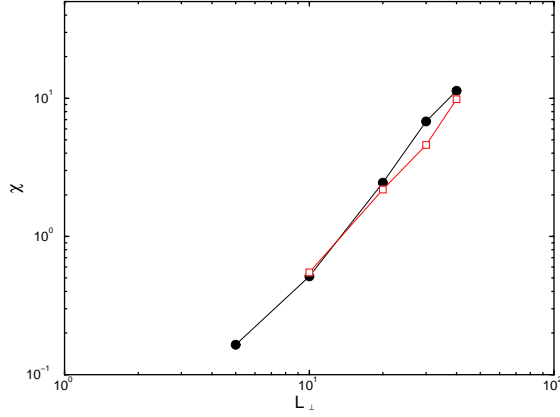


FIG. 9. The susceptibility  $\chi$  at  $T_c$  in the limit  $L_{\parallel} \rightarrow \infty$  as a function of the perpendicular dimension  $L_{\perp}$  in logarithmic scales. The critical temperature used is  $T_c = 4.860$  for the circles and  $T_c = 4.872$  for open squares.

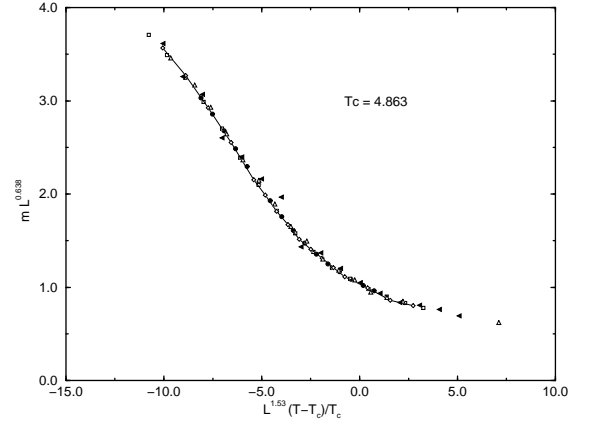


FIG. 11. Scaling of the magnetization for the cubic systems. The linear sizes are 20 (solid circle), 30 (square), 40 (diamond), 50 (open triangle), 60 (solid triangle).

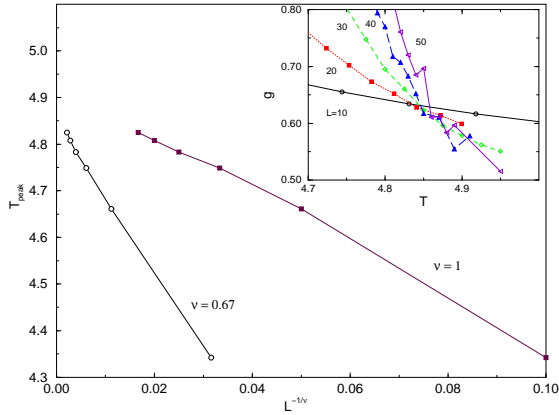


FIG. 10. The location of the susceptibility peak v.s.  $L^{-1/\nu}$  for  $\nu = 0.67$  and 1. The insert shows the intersections of the fourth order cumulant  $g$  between different  $L$ .

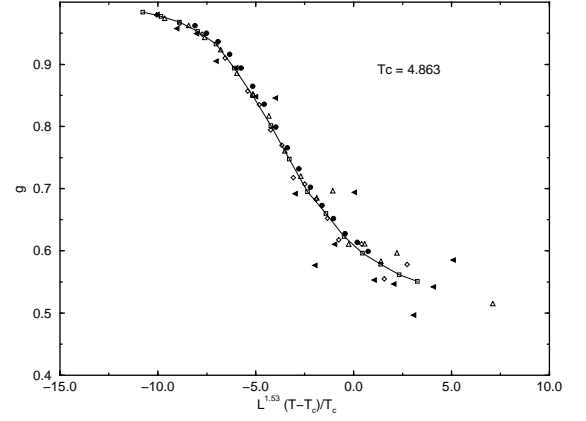


FIG. 12. Scaling of the fourth order cumulants for the cubic systems. The system sizes are the same as in the previous figure.

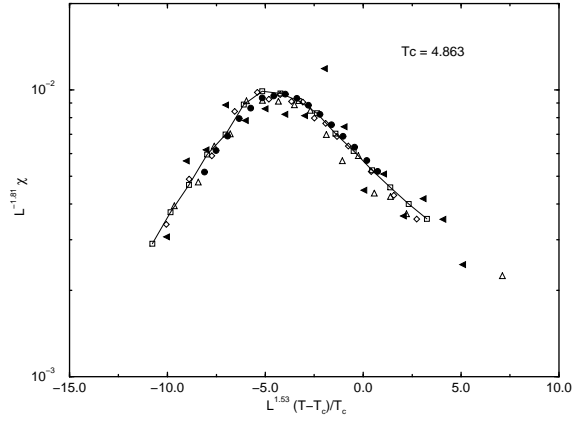


FIG. 13. Scaling of the susceptibility for the cubic systems. The system sizes are the same as in the previous figure.

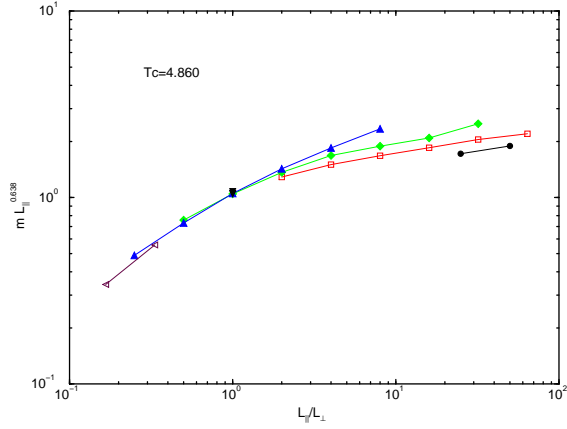


FIG. 14. Isotropic scaling for magnetization at  $T_c$ , using the same set of original data as in Fig. 7.